Coastal Engineering 156 (2020) 103613

Contents lists available at ScienceDirect

Coastal Engineering

journal homepage: http://www.elsevier.com/locate/coastaleng

The influence of a berm and roughness on the wave overtopping at dikes

W. Chen [a,b,*], M.R.A. van Gent [b], J.J. Warmink [a], S.J.M.H. Hulscher [a]

[a] Department of Marine and Fluvial Systems, University of Twente, Drienerlolaan 5, 7522 NB, Enschede, the Netherlands
[b] Department of Coastal Structures & Waves, Deltares, Boussinesqweg 1, 2629 HV, Delft, the Netherlands

ARTICLE INFO

Keywords:
Overtopping discharge
Berm
Block revetment
Varying roughness
Laboratory experiments

ABSTRACT

A reliable estimation of average wave overtopping discharge is important for dike design and safety assessment. Berms and roughness elements are widely applied to reduce the overtopping discharge over dikes. In this study, the effects of a berm and roughness on the wave overtopping discharge are investigated by means of physical model tests. New empirical formulae are derived from the analysis of the experimental data in order to provide more accurate estimations of reductive influence of berms and roughness on the wave overtopping discharge. Additionally, a new formula is developed to estimate the reductive influence of varying roughness along the waterside slopes with a berm. The new equations show a significantly better performance within the tested range when compared with existing formulae for the average overtopping discharge.

1. Introduction

Many coastal societies face increasing risks of coastal flood disasters as a result of climate change, sea level-rise and land subsidence (Borsje et al., 2011; Temmerman et al., 2013). Dikes are important coastal structures to protect infrastructure and people in coastal areas from storms (see for instance Goda, 2009). The average wave overtopping is often used to determine the required crest level and cross-section geometry of dikes by ensuring that the average overtopping discharge is below acceptable limits under specified design conditions. Therefore, a reliable prediction of the average overtopping discharge is essential for dike design and reliability (see also Jafari and Etemad-Shahidi, 2011).

Empirical formulations of average overtopping discharge have been a key tool used in the design of the crest level of coastal structures. TAW (2002) provides overtopping equations for breaking and non-breaking waves at dikes that are adopted in EurOtop (2007) to calculate the average overtopping discharge taking several influence factors (i.e. roughness, berms, oblique waves, vertical wall) into account (Appendix A.1). In these formulae, all influence factors affect the overtopping discharge of the breaking waves while the overtopping discharge of the non-breaking conditions is only affected by the revetment roughness and oblique waves. EurOtop (2018) adapted the TAW (2002) overtopping expression especially for low freeboards, including the zero freeboard. The formulae provided by EurOtop (2018) are similar to those by TAW (2002) but have a power function in the exponent and different values for the empirical coefficients. The same influence factors are adopted in EurOtop (2018) as those in TAW (2002) but to a different power (1.3) (See Table A.1 in Appendix A.1). Gallach-Sánchez (2018) calibrated the power coefficient for relative free board $R_c/H_{m0} \geq 0$ based on more extensive tests and the calibrated value of the power coefficient is 1.1 instead of 1.3. Hence, there is still some dispute over the optimal value for the power coefficient. Capel (2015) derived an overtopping equation on the basis of the wave run-up on dikes. This equation is applicable to both breaking and non-breaking waves. The above mentioned empirical overtopping estimators are summarised in Appendix Table A.1.

In practical engineering, berms and roughness elements are often applied to reduce the average overtopping discharge. In these empirical overtopping formulae, the amount of wave overtopping is affected by berms and by the roughness of the slope covers that are parameterized as influence factors.

There have been some methods available to estimate the berm influence. TAW (2002) and EurOtop (2007, 2018) recommend a method to calculate the berm influence factors as a function of the berm width and berm level relative to the still water level (Eq. (A.3)). Instead of introducing a berm factor, Van Gent (1999) includes the berm influence through a characteristic slope which refers to the mean slope of the waterside slopes taking the berms into account. This method assumes that the berm position relative to the SWL has no effect on the overtopping discharge when the berm is located between $2H_{m0}$ above and $-2H_{m0}$ below the still water line. However, these research are limited to

* Corresponding author. Department of Marine and Fluvial Systems, University of Twente, Drienerlolaan 5, 7522 NB, Enschede, the Netherlands.
E-mail addresses: w.chen-6@utwente.nl (W. Chen), Marcel.vanGent@deltares.nl (M.R.A. van Gent), j.j.warmink@utwente.nl (J.J. Warmink), s.j.m.h.hulscher@utwente.nl (S.J.M.H. Hulscher).

https://doi.org/10.1016/j.coastaleng.2019.103613
Received 18 March 2019; Received in revised form 5 September 2019; Accepted 1 December 2019
Available online 4 December 2019

Table 1
Summary of parameters of the datasets.

Dataset		R_c [m]	d_h [m]	H_{m0} [m]	$s_{m-1,0}$ [−]	$\xi_{m-1,0}$ [−]	q^*	Number
Set1	S-REF	(0.12, 0.18)*	-	(0.09, 0.123)	(0.027, 0.049)	(1.50, 2.03)	(0.001, 0.016)	62
	S-PB	(0.12, 0.18)	–	(0.09, 0.123)	(0.027, 0.049)	(1.50, 2.03)	(1e-4, 0.0076)	62
	S-OB	(0.12, 0.18)	–	(0.09, 0.123)	(0.027, 0.049)	(1.50, 2.03)	(1e-4, 0.006)	62
Set2	B-REF	(0.12, 0.18)	(-0.03, 0.03)	(0.09, 0.133)	(0.027, 0.040)	(1.67, 2.03)	(3e-4, 0.009)	47
	PB3	(0.12, 0.18)	(-0.03, 0.03)	(0.09, 0.133)	(0.027, 0.040)	(1.67, 2.03)	(1e-4, 0.003)	20
	OB3	(0.12, 0.18)	(-0.03, 0.03)	(0.09, 0.133)	(0.027, 0.040)	(1.67, 2.03)	(1e-4, 0.0023)	20
Set3	PB1	(0.12, 0.18)	(-0.03, 0.03)	(0.1, 0.133)	(0.027, 0.042)	(1.63, 2.03)	(1e-4, 0.003)	25
	PB2	(0.12, 0.18)	(-0.03, 0.03)	(0.1, 0.133)	(0.027, 0.042)	(1.63, 2.03)	(7e-5, 0.003)	25
	OB2	(0.12, 0.18)	(-0.03, 0.03)	(0.1, 0.133)	(0.027, 0.042)	(1.63, 2.03)	(6e-5, 0.002)	25
Set4	OB1	(0.12, 0.18)	(-0.03, 0.03)	(0.09, 0.12)	(0.027, 0.042)	(1.63, 2.03)	(4e-5, 0.002)	27
	OB2-d	(0.12, 0.18)	(-0.03, 0.03)	(0.09, 0.12)	(0.027, 0.042)	(1.63, 2.03)	(4e-4, 0.008)	27
	COM	(0.12, 0.18)	(-0.03, 0.03)	(0.09, 0.12)	(0.027, 0.042)	(1.63, 2.03)	(5e-5, 0.0034)	27
				Total number				429

* () in Table 1 represents interval.

impermeable berms. Thus, a suitable method to take the influence of permeable berms of dikes into account is not available.

According to the literature, most of the research on roughness elements use constant values of the roughness factor to account for the roughness influence on the wave overtopping discharge. TAW (2002) and EurOtop (2007, 2018) provide default values of roughness influence factors for a large variety of roughness elements in breaking wave conditions. For non-breaking waves, roughness factors are slightly affected by the breaker parameter (Eq. (A.6)). Bruce et al. (2009) measured the relative difference in mean overtopping discharge for various types of armour units and presented the roughness factor values for various types of roughness elements. Those static roughness values were then used in the neural network prediction of overtopping (e.g., Van Gent et al., 2007; Verhaeghe et al., 2008). Nevertheless, Capel (2015) and Van Steeg et al. (2018) have shown that the roughness factors are not constant for breaking waves but that they depend on other parameters such as wave conditions and dike configurations. Capel (2015) studied the effect of the roughness of blocks with protrusion on wave overtopping and wave run-up and proposed a new equation to assess the roughness influence coefficient of protruding blocks (Eq. (A.7)). The results showed that the effect of roughness decreased with the increasing mean overtopping discharges. Capel (2015) also showed that the wave steepness at the toe of the structure also has an influence on the roughness factor that is not influenced by the slope. A new parameter, roughness density is introduced to describe the characteristics of the roughness pattern. The Capel (2015) formula improves overtopping discharge predictions for straight slopes covered by protruding blocks. However, this equation needs iteration to calculate the roughness factors and is therefore somewhat complicated when applying to practical engineering. Moreover, various types of roughness elements are often combined in the slope protection of dikes. For the varying roughness along the slopes and berms, the various influence factors are weighted in TAW (2002) by including the lengths of the relevant sections of the slope. If three types of roughness elements with lengths of L_1, L_2 and L_3 and influence factors of $\gamma_{f,1}$, $\gamma_{f,2}$ and $\gamma_{f,3}$ respectively are applied along the slopes and berms, then the weighted average as proposed by TAW (2002) is:

$$\gamma_f = \frac{\gamma_{f,1}L_1 + \gamma_{f,2}L_2 + \gamma_{f,3}L_3}{L_1 + L_2 + L_3} \tag{1}$$

This equation is the only available method to estimate the influence of a combination of various types of roughness elements along the

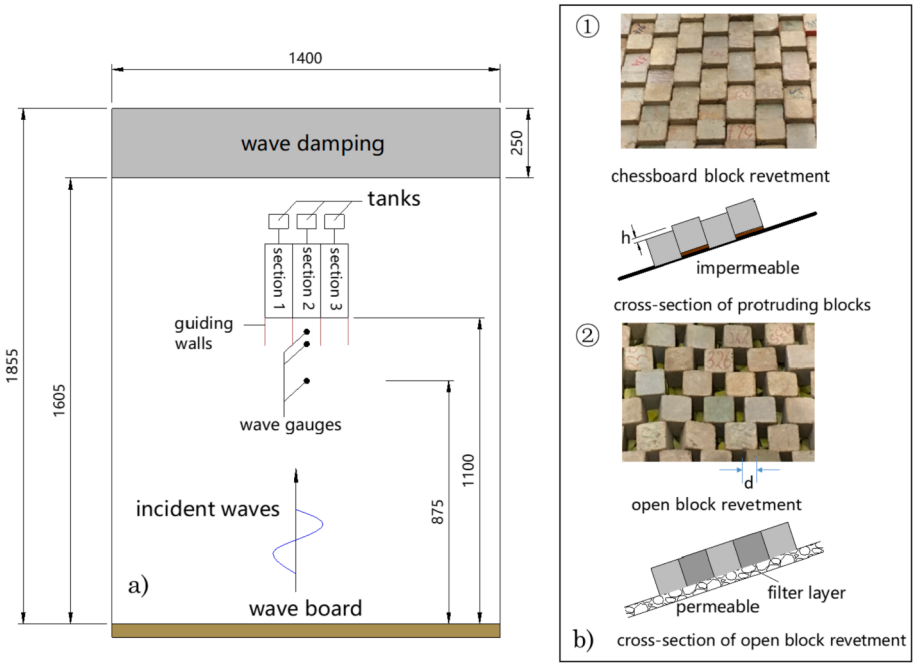

Fig. 1. Overview layout of tested models with a) top view layout of test conditions (unit: cm); and b) roughness elements with ① the protrusion height $h = 1cm$ and ② $d = 2cm$ and thickness of the filter layer is 2.5 cm with $D_{n50} = 2.5$ cm.

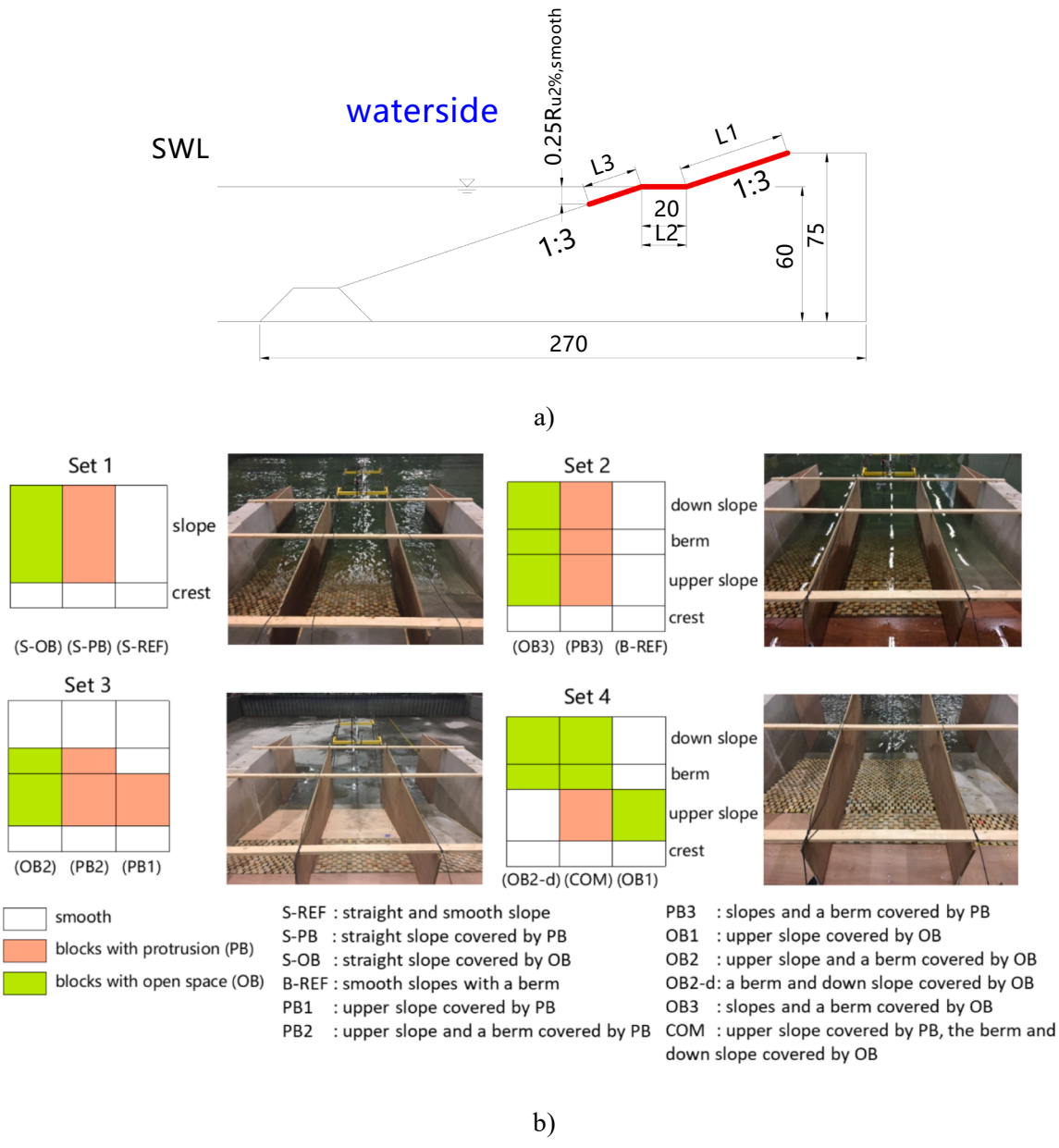

Fig. 2. Schematic diagram of a) cross-section of tested slopes with a berm (unit: cm) and b) tested configurations with different types of roughness elements.

slopes. However, Eq. (1) has not been validated systematically and therefore the accuracy of this formula remains unknown.

To summarise, existing methods to take the influence of berms and roughness into account still need improvement. Also, the combined influence of a berm and roughness on the wave overtopping discharge is poorly studied and the only currently available method has not been validated systematically against experimental data. Therefore, the goal of this study is to gain insight into the effects of berms and roughness on wave overtopping at dikes and to increase the prediction accuracy of the average overtopping discharge by improving the methods for estimating roughness and berm influence.

In the present study, physical model tests have been conducted to investigate the influence of a berm and roughness on the average overtopping discharge. Effects of the wave height and wave steepness, the dike configurations and the permeability are analysed to assess the influence of roughness and berms. After the influence factors of roughness and berms have been analysed, the combined influence of varying roughness along the slopes and berms are studied.

The physical model tests have been presented in Section 2. In Section 3, the analysis of the test results is described, including the introduction of new empirical formulae. In Section 4, a further discussion of the results is provided. In Section 5, the main conclusions of the presented research are summarised.

2. Physical model tests

2.1. Experimental facilities

Physical model tests were performed in the Pacific Basin at Deltares in The Netherlands. This basin is 18.6 m long, 14 m wide and 1.25 m deep (Fig. 1a). To minimize the influence of reflected waves by the test section with a width of 3 m, a passive permeable wave damping slope has been applied over the full width of the wave basin. A second-order wave control was used to reduce the generation of spurious waves. In the present physical model tests, irregular waves based on the JONSWAP spectrum that has a peak enhancement factor of 3.3 were generated with different combinations of significant wave heights and periods. Three wave gauges were placed near the toe of the structure to

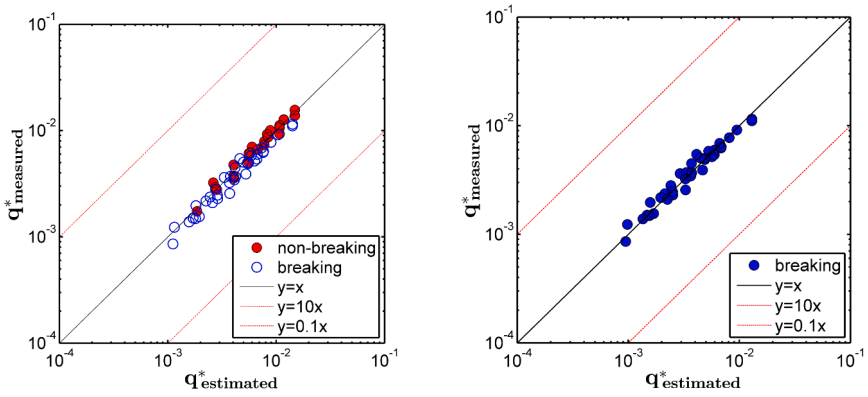

a) TAW equations b) Recalibrated TAW equation

Fig. 3. Measured dimensionless overtopping discharges versus estimated ones using a) TAW equations; and b) recalibrated TAW equation for breaking waves (Dataset S-REF).

measure the wave conditions. Incident and reflected waves were separated by using the method proposed by Mansard and Funke (1980). The wave conditions, including the spectral significant wave height H_{m0} and the mean energy wave period $T_{m-1,0}$, were obtained from the analysis of the measured incident waves at the toe of the structure.

2.2. Model set-up

The wave basin is wide enough to allow three model sections to be tested simultaneously. The width of each section was 1.0 m. The core of the structures were all impermeable and is made of concrete. Plywood is detachable to be freely placed on the impermeable core as a smooth slope or to be removed to install blocks. Wooden boards were installed between the tested models to avoid the influence of adjacent sections. The overtopped water was led into the overtopping tanks by using chutes placed at the rear edge of the crest. One wave gauge was installed in each tank to detect the variations of the water level, which enables the measurement of the overtopped water volume. Both straight slopes without a berm and slopes with a berm were tested in this test programme. Three types of slope protection were considered in the tests: (1) protruding blocks (closed without open space); (2) open blocks without protrusion; (3) smooth slopes representing asphalt or grass. Applying the hypothetical geometrical model scale of 1:15, cubes of 50 mm represented about the size of 0.75 m × 0.75 m at the prototype scale. The chessboard pattern of protruding blocks was created by placing a concrete tile of 10 mm thick underneath the blocks such that the protrusion equals the thickness of the concrete tile (Fig. 1b-①). Open blocks were placed on the filter layer with a thickness of 2.5 cm leaving small gaps between the blocks (Fig. 1b-②). The filter layer was placed directly on the smooth impermeable core. Previous research (Van Gent et al., 1999) showed that open space should be 25–30% (percentage of the volume of spaces between blocks divided by the total control volume) of the armour layer to obtain a reasonably stable revetment. Hence, 30% open space was used in the tests, which represents a suitable compromise between stability and the amount of blocks needed, resulting in the gap $d = 2$ cm. A slope of 1:3 which is a typical dike slope was used for the straight slopes as well as for the upper slope and for the down slope of sections that have a berm (Fig. 2a). The structures were constructed such that the external boundaries of the slopes, excluding potential protruding parts, determine the slope parameters. Note that the highest points of the protruding blocks in the upper row may be slightly higher than the crest level. In Fig. 2a, L_1, L_2 and L_3 represent the effective coverage length of roughness elements on the upper slope, berm and down slope respectively, which is further explained later. A berm width of 0.20 m was applied (i.e. the total width of four blocks).

Various types of roughness elements and different configurations including straight slopes (S) and composite slopes with a berm (B) were combined resulting in four sets of sections (Fig. 2b). The applied locations of the blocks along the slopes were varied. Numbers in the codes of these sections represent (1) upper slope, (2) upper slope and the berm and (3) entire surface. OB2-d represent the section with open blocks applied on the berm and down slope. COM denotes the combination of protruding blocks (PB) and open blocks (OB) applied on the surface simultaneously. Blocks on the down slope are installed along the entire down slope from the toe to the berm.

2.3. Test programme

For each tested section, the berm position as shown in Fig. 2a was fixed during the tests. Therefore, the berm level relative to the still water level only varies with changes in the water depth. Five freeboards were investigated by changing the water depth by 0.015 m for each test run. For each freeboard, the wave height H_{m0} and spectral wave period $T_{m-1,0}$ were varied resulting in the variation of the wave steepness $s_{m-1,0}$. The ranges of those parameters that were varied in this test programme are listed in Table 1, where R_c (0.12 m, 0.135 m, 0.15 m, 0.165 m and 0.18 m) is the relative freeboard, d_h (-0.03 m, −0.015 m, 0 m, 0.015 m, 0.03 m) is the water depth above the berm, $\xi_{m-1,0}$ is the breaker parameter (Iribarren parameter) and q^* ($= \frac{q}{\sqrt{gH_{m0}^3}}$) is the non-dimensional average overtopping discharge. Wave overtopping for each test was measured for at least 1000 waves. This time duration is considered sufficient for generating the full wave height and period distribution over the frequency domain of interest and for stabilizing statistical properties of wave overtopping. In total, 429 tests were conducted.

3. Analysis of experimental results

Since the TAW (2002) overtopping equations are still the most used methods for predicting the average overtopping discharge (Capel, 2015), the TAW equations are estimated and recalibrated using the data from the reference tests (Dataset S-REF) performed on smooth straight slopes. Once the structure profile is defined and wave conditions and overtopping discharge are known, the recalibrated TAW (2002) overtopping equations can serve as reference equations to calculate the effective roughness factors in case of no berm ($\gamma_b = 1$) and berm factors with no roughness ($\gamma_f = 1$) based on the experimental data. Regression analysis is conducted for effective berm and roughness coefficients, showing that the roughness factor varies with wave conditions and berm factor is also affected by wave steepness apart from berm geometry and location. The efficiency of the new formulae for berm and roughness

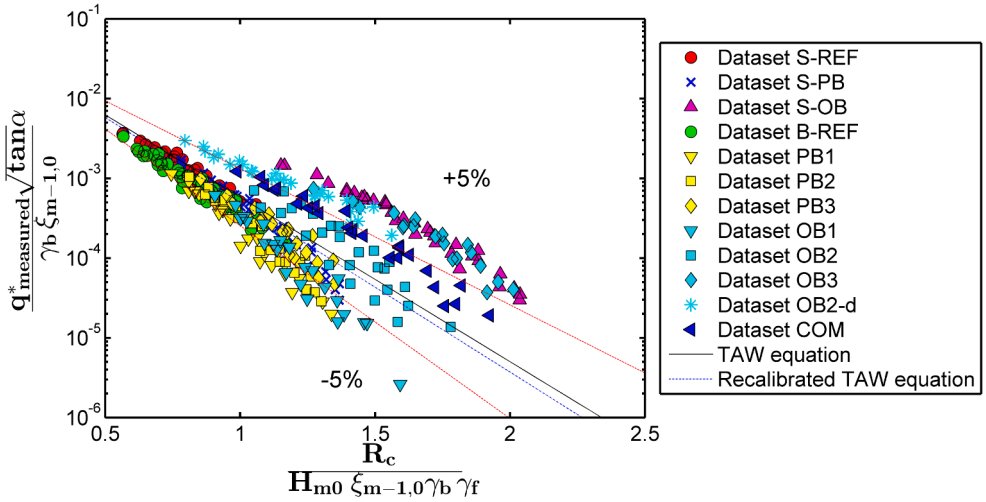

a) Breaking wave conditions

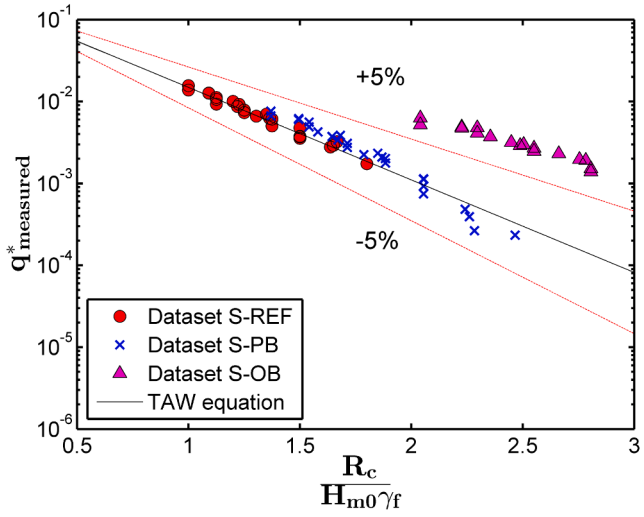

b) Non-breaking wave conditions

Fig. 4. Wave overtopping data for a) Breaking wave conditions; and b) Non-breaking wave conditions with the 5% exceedance lines (red dash lines) indicating the 90% confidence band of the TAW equations.

coefficients obtained by regression are then compared with TAW (2002) formulae. The case in which a berm and roughness are combined is then analysed and different solution methods are proposed for impermeable and permeable berms. Finally, the varying roughness along the surface is analysed and weights are derived to combine roughness coefficients of different types of roughness elements on upper slope, berm and down slope.

3.1. Recalibration of TAW (2002) overtopping formulae

Measured overtopping discharges for smooth straight slopes were compared against calculated discharges using the TAW overtopping formulae (Eq. (A.1, A.2)) (Fig. 3a). The results show that the equation (Eq. (A.1)) for non-breaking waves predicts the overtopping discharges of smooth straight slopes quite well. However, the equation (Eq. (A.2)) for breaking waves slightly overestimates the overtopping discharges. Hence, for the analysis, this equation is recalibrated based on the present dataset. This was achieved by recalibrating the coefficient −4.75 in the equation for breaking waves to −4.90 through fitting the experimental data (Dataset S-REF) by applying the least squares method. To check the performance of the recalibrated equation for breaking waves (Eq. (2)), the calculated and measured overtopping discharges were compared and a good agreement was found as shown in Fig. 3b. The recalibrated new equation (i.e. Eq. (2)) has a mean relative error (MRE) of 9.7%, which is smaller than the MRE of 15.6% for the TAW equation for breaking waves:

$$q^* = \frac{0.067}{\sqrt{\tan\alpha}}\gamma_b\xi_{m-1,0}\exp\left(-4.90\frac{R_c}{H_{m0}\xi_{m-1,0}\gamma_b\gamma_f\gamma_\beta\gamma_v}\right) \quad (2)$$

where $\gamma_\beta = \gamma_v = 1$ in this study, and $q^* = \frac{q}{\sqrt{gH_{m0}^3}}$.

The wave overtopping data of the tests for all sections, the TAW equations and the recalibrated TAW equation for breaking waves are plotted in Fig. 4. This was done for both the breaking wave conditions and non-breaking wave conditions. TAW method (Eq. (A.3)) is adopted to calculate the berm factors. Roughness coefficient γ_f of 0.73 for protruding blocks is given by EurOtop (2018) and the value 0.49 for single

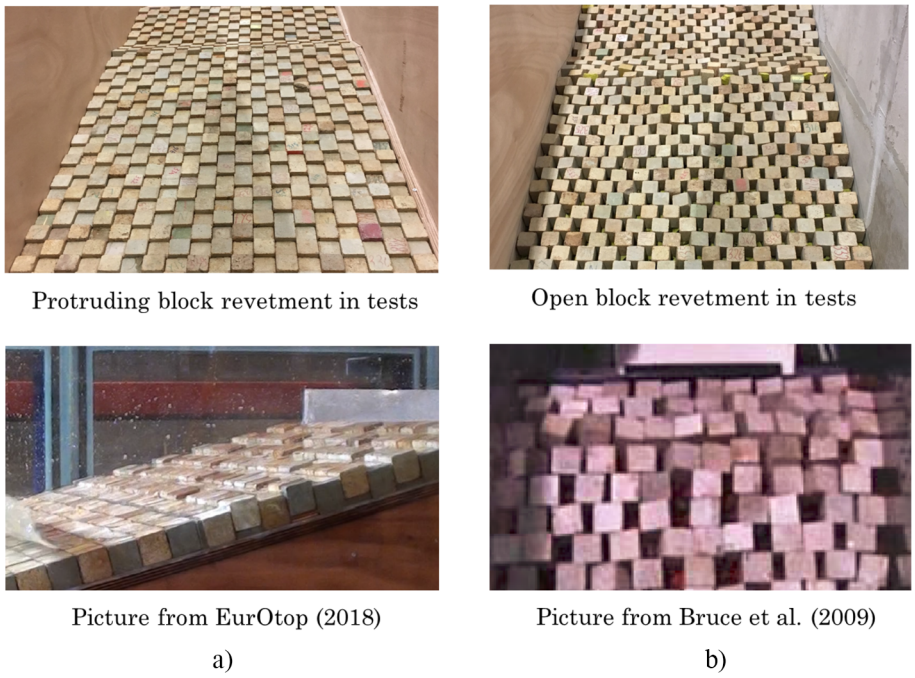

Fig. 5. Comparison of rough slopes with those provided in previous literature with a) protruding block revetment and b) open block revetment.

layer of open blocks is given by Bruce et al. (2009) and also EurOtop (2018). The comparisons of roughness revetments applied in the tests with those from previous literature (Bruce et al., 2009; EurOtop, 2018) are present in Fig. 5. Even though the recalibrated equation (2) predicts the overtopping discharge of smooth straight slopes rather good, Fig. 4 shows large and systematic differences for the various dike geometries. These differences are caused by the TAW equations (A.3) and (A.6) failing to accurately estimate the berm influence and roughness influence factors.

The points from the Dataset S-OB show that the roughness influence is considerably overestimated by the TAW method. This might be, because the γ_f of 0.49 for open block roughness is obtained based on the tests on breakwaters with a permeable core. Thus, this value, which is recalibrated later using Dataset S-OB, may not be reasonable for dikes with an impermeable core. The influence of protruding blocks is estimated reasonably for non-breaking conditions while it is somewhat underestimated for conditions with breaking waves (see Dataset S-PB points). Additionally, the data for section B-REF (green circles in Fig. 4a) lie below the TAW equation line, which indicates that the berm influence is underestimated. The roughness factors were calculated by using Eq. (1) for the sections that had various types of roughness elements applied. The differences between the measured and calculated overtopping discharges demonstrate that Eq. (1) cannot accurately predict the reductive influence of varying roughness along the slopes with a berm. Therefore, it is necessary to improve the TAW equations for estimating the influence of a berm and roughness distribution on the average overtopping discharge.

3.2. *Results for protruding blocks*

In subsection 3.2.1, the effective roughness factors of protruding blocks on the straight slope are obtained by directly solving the overtopping formulae with the average overtopping discharge (q) substituted by the measured overtopping discharge (Dataset S-PB). Both equations for breaking waves and non-breaking waves include the roughness coefficient. Therefore, Eq. (2) is used to calculate the effective roughness factors for $\xi_{m-1,0}<1.8$ and the TAW equation for non-breaking waves (Eq. (A.2) in the Appendix) is used for $\xi_{m-1,0}>1.8$. Similarly, the

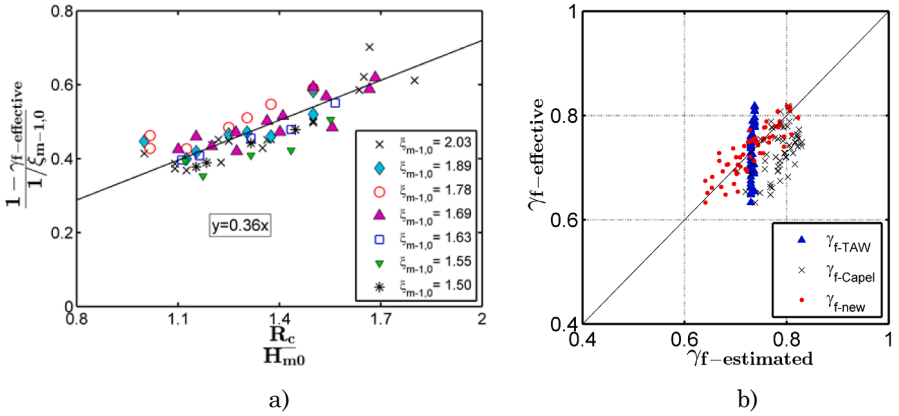

Fig. 6. Analysis of roughness factors of protruding blocks on the straight slope (Dataset S-PB) with: a) Influence of relative free board and breaker parameter on roughness influence factors; and b) Comparison of effective roughness factors and calculated roughness factors using TAW method, the Capel (2015) method and the new equation (Eq. (3)).

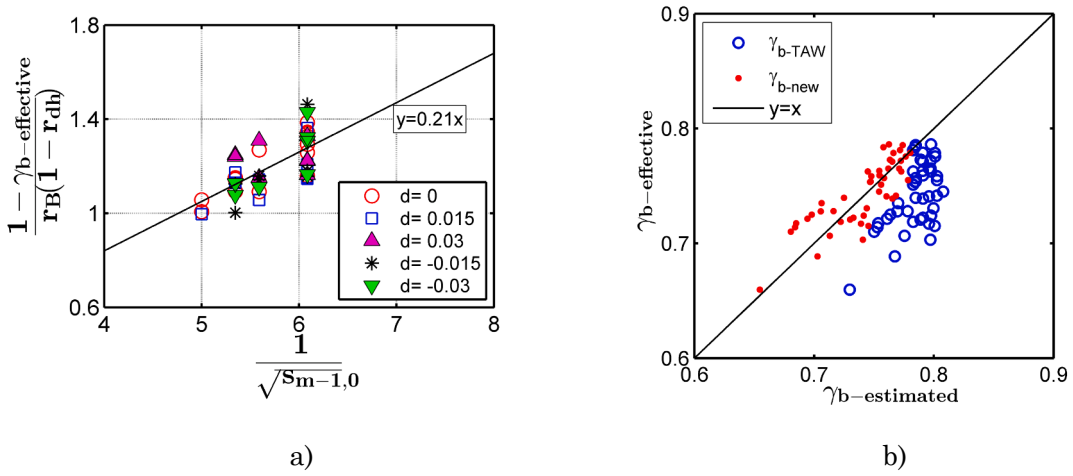

Fig. 7. Analysis of impermeable berm factors using Dataset B-REF with: a) Influence of wave steepness on influence factors of an impermeable berm; and b) Comparison of effective berm factors with estimated factors using TAW (2002) equation and new equation (Eq. (5)).

breaking equation (Eq. (2)) was used as the basis of calculation of effective impermeable berm factors (Dataset B-REF) as presented in subsection 3.2.2. With the effective influence factors available, it is feasible to fit the experimental data and to derive new equations for roughness and berm effect factors. The newly derived equations are validated by comparing the estimated values with the effective influence factors obtained from the measured overtopping discharges. Subsection 3.2.3 deals with the roughness influence of protruding blocks applied on parts of the dike surface.

3.2.1. *Roughness influence of protruding blocks on the straight slope*

The effective roughness factors $\gamma_{f-effective}$ and dimensionless parameters R_c/H_{m0} and $\xi_{m-1,0}$ are plotted in Fig. 6a with on the vertical axis the, for breaker parameter corrected, roughness factor '$(1-\gamma_{f-effective})/(1/\xi_{m-1,0})$' and on the horizontal axis the relative freeboard 'R_c/H_{m0}'. We use R_c/H_{m0} because the overtopping discharge is most sensitive to the relative freeboard when $R_c/H_{m0}>1$ (Pillai et al., 2017) and the roughness factor is affected by overtopping discharge (Capel, 2015). The data show a linear relation between these two terms. As the relative freeboard increases, the roughness influence increases (i.e. a lower reduction factor due to roughness). This can be explained as follows: the roughness has more effect for conditions with a thinner layer thickness, which is the case for larger relative freeboards with less overtopping. In addition to the influence of the relative freeboard, conditions with a smaller breaker parameter also show an increase of the influence of the roughness (i.e. a lower reduction factor due to roughness). The linear relation in Fig. 5a results in a new equation for roughness factors of protruding blocks by using the linear regression method:

$$\gamma_f = 1 - \frac{c_0 R_c}{H_{m0}\xi_{m-1,0}} \tag{3}$$

where $c_0 = 0.36$. It is feasible to calibrate the coefficient c_0 for other types of roughness elements on straight slopes. Note that the slope is not varied in the tests and therefore the breaker parameter $\xi_{m-1,0}$ is strictly related to wave steepness.

The estimated roughness factors ($\gamma_{f-estimated}$) by using TAW method (Eq. (A.6)), Capel equation (7) and the new equation (3) were compared with the effective roughness factors ($\gamma_{f-effective}$) (Fig. 6b) to validate the performance of the new equation that estimates the roughness influence of protruding blocks. The Nash–Sutcliffe model efficiency coefficient (NSE) is used to assess the predictive power of the empirical formulae and is defined as:

$$NSE = 1 - \frac{\sum_{i=1}^{N}(x_i - y_i)^2}{\sum_{i=1}^{N}(x_i - \bar{x})^2} \tag{4}$$

where N is the number of observations; x_i is the observed value; $\bar{x}$ is the mean value of the observed data; y_i is the predicted value. NSE can range from $-\infty$ to 1. $NSE = 1$ corresponds to a perfect match of predicted data to the measured data. $NSE = 0$ indicates that the predicted values are as accurate as the mean of the measured data. $NSE < 0$ indicates that the observed mean is a better predictor than the empirical formula. The closer the *NSE* is to 1, the more accurate the empirical formula is.

The results show that the developed equation can estimate the roughness influence much better than the TAW (2002) and Capel (2015) equations with NSE improving from 0.07 for the TAW (2002) equation and −1.13 for the Capel equation to 0.71 for the new equation (3).

3.2.2. *Influence factor of an impermeable berm*

Dataset B-REF is used to investigate the reductive influence of an impermeable berm on the average overtopping discharge. Since the data on non-breaking waves are close to the transition from breaking waves to non-breaking waves and adding a berm would cause that the waves are more breaking than surging (Van Gent, 2013), the breaking equation (2) was used as the basis of calculation of effective berm factors by applying $\gamma_f = \gamma_\beta = \gamma_v = 1$ (i.e. the influence factors for roughness, oblique waves and vertical walls, respectively, all set at no influence). Plotting the inverse of the root square of the wave steepness '$1/\sqrt{s_{m-1,0}}$' on the horizontal axis and the changed berm factors '$(1-\gamma_{b-effective})/(r_B(1-r_{dh}))$' on the vertical axis (where r_B is a parameter taking the width of the berm into account and r_{dh} is a parameter to take the level of the berm into account) shows that wave steepness has an effect on the berm factors (Fig. 7a). The berm influence increases as the wave steepness decreases. A modified equation (5) for impermeable berm factors was developed by fitting the experimental data:

$$\gamma_b = 1 - b_0\frac{r_B(1-r_{dh})}{\sqrt{s_{m-1,0}}} \quad 0.6 \le \gamma_b \le 1.0 \tag{5}$$

with the expressions for r_B and r_{dh} from TAW (2002):

$$r_B = \frac{B}{L_{Berm}}$$

$$r_{dh} = 0.5 - 0.5\cos\left(\pi\frac{d_h}{R_{u2\%}}\right) \text{ for a berm above the still water level}$$

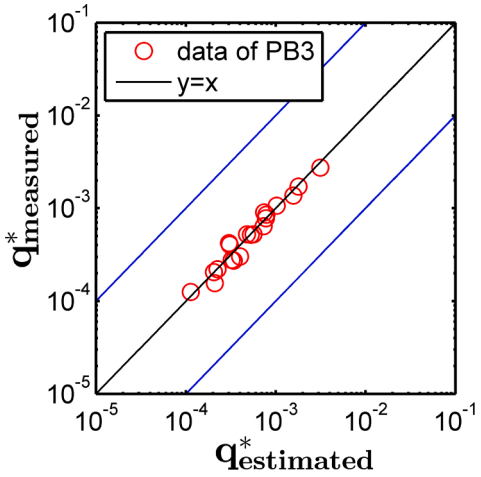

Fig. 8. Measured versus estimated overtopping discharges over section PB3 that has protruding blocks applied on the slopes and the berm. The berm and the roughness influence factors are calculated by using Eq. (5) and by using Eq. (3) respectively.

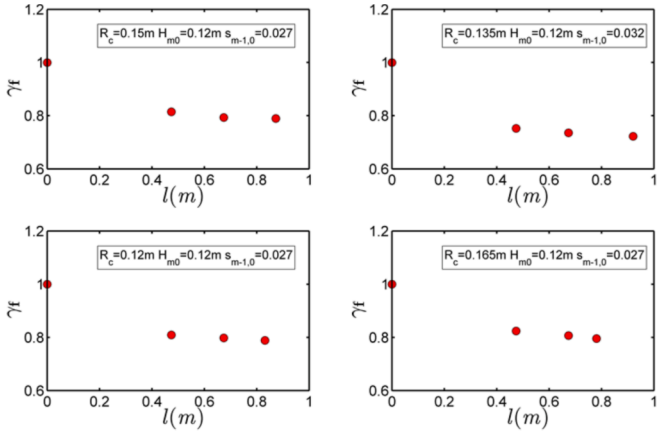

Fig. 9. Comparison of roughness factors of the slopes for four test conditions selected from Datasets PB1, PB2 and PB3.

$$r_{dh} = 0.5 - 0.5\cos\left(\pi\frac{d_h}{2{\cdot}H_{m0}}\right) \quad \text{for a berm below the still water level}$$

where the empirically derived coefficient b_0 is 0.21. $r_B[-]$ represents the influence of the berm width B [m]and $r_{dh}[-]$ stands for the effect of the d_h[m] which refers to position of the berm relative to SWL; $R_{u2\%}$ is the wave run-up height that is exceeded by 2% of the number of incoming waves at the toe of the structure, which can calculated using Eq. (A.4, A.5). The maximum influence is limited to $\gamma_b = 0.6$ (EurOtop, 2018), which is also adopted in the new Eq. (5).

Fig. 7b shows that the estimated berm factors by using Eq. (5) increases the NSE from −1.91 for TAW (2002) Eq. (A.4) to 0.60 for the new equation. It must be mentioned that Eq. (5) is developed for impermeable berms only, which are the smooth berms (B-REF) and berms covered with protruding blocks. The influence factors for a permeable berm covered by open blocks will be discussed later.

3.2.3. *Combined influence of a berm and roughness for protruding blocks*

Eq. (5) is assumed to be applicable for a berm covered by protruding blocks since the protruding block revetment is impermeable. Eq. (3) for roughness influence factors and Eq. (5) for berm factors are used in combination to calculate the combined influence $\gamma_b\gamma_f$ for Dataset PB3. With this combined influence known, the average overtopping discharges are calculated using Eq. (2), and are then compared with the measured ones from Dataset PB3 (Fig. 8). The results show that there is good agreement between estimated and measured overtopping discharges, which suggests that Eq. (3) for the roughness influence is also valid for the slopes with a berm.

Datasets PB1, PB2 and PB3 are selected to investigate the reductive influence of varying roughness along the slopes that have a berm. Effective roughness factors of section PB1, PB2 and PB3 are calculated on the basis of Eq. (2) with berm factors being obtained using Eq. (5) and $\gamma_\beta = \gamma_v = 1$. Fig. 9 shows the effective roughness factor data for protruding blocks on parts of the slopes that have a berm under various test conditions in terms of total coverage length of protruding blocks l (m) on the horizontal axis and effective roughness factor γ_f on the vertical axis.

The four points from left to right in each scatter diagram in Fig. 9 represent the effective roughness factors of sections B-REF, PB1, PB2 and PB3 respectively. The values of the roughness factor significantly decrease from smooth slopes (B-REF) where $\gamma_f = 1$ for $l = 0$m to slopes that have blocks on the upper slope (PB1) where $\gamma_f \approx 0.8$. However, the decrease of the roughness factor is small if the blocks are also applied to the berm and down slope. Therefore, blocks on the upper slope are effective while the blocks on the berm and down slope have only a limited effect on the total roughness influence. This can be explained as follows: the water layer thickness becomes much smaller on the upper slope than on the berm and on the down slope, and therefore the roughness influence becomes more pronounced for the upper slope. Blocks on various parts of the slopes contribute differently to the total roughness factor, which demonstrates that the TAW (2002) equation for calculating varying roughness along the slopes is not accurate since the calculated roughness factor using Eq. (1) decreases linearly as the coverage length increases. To describe the contributions of blocks on various parts of the surface (Fig. 2a) (between $0.25R_{u2\%,smooth}$ under the still water line and the crest in this study) to the total roughness factor, location weighting coefficients are introduced for various parts of the waterside surface. The roughness elements placed below $0.25R_{u2\%,smooth}$ under the still water level have little or no effect on the total roughness factor (TAW, 2002)). Therefore, only the roughness elements lying between $0.25R_{u2\%,smooth}$ under the still water level and the crest are taken into account to calculate the roughness influence factor. Accordingly, L_3 in Fig. 2a is the effective coverage length above the $0.25R_{u2\%,smooth}$ under the still water level. $R_{u2\%,smooth}$ is the wave run-up on a smooth surface which can be calculated by using Eq. (A.4, A.5) (Appendix A.2), with $\gamma_f = 1$. Consequently, the effective coverage length L_3 varies with wave conditions, because the location of wave impact on the slope changes with hydrodynamic conditions. Eq. (1) is modified to:

$$\gamma_f = \frac{\alpha_1\gamma_{f,1}L_1 + \alpha_2\gamma_{f,2}L_2 + \alpha_3\gamma_{f,3}L_3}{\alpha_1L_1 + \alpha_2L_2 + \alpha_3L_3} \tag{6}$$

where α_1, α_2 and α_3 are the location-weighting coefficients for roughness elements on the upper slope, berm and down slope respectively and $\alpha_1 + \alpha_2 + \alpha_3 = 1$. $\gamma_{f,1}$, $\gamma_{f,2}$ and $\gamma_{f,3}$ are the roughness factors of roughness elements applied over the entire surface. L_1, L_2 and L_3 are the effective coverage lengths of roughness elements as shown in Fig. 2a.

For each test condition, the values of α_1, α_2 and α_3 can be obtained by solving Eq. (6). Applying this procedure yields the mean values of α_1, α_2 and α_3 of 0.65 (±0.116), 0.22 (±0.062) and 0.13 (±0.071) for upper slope, berm and down slope respectively. The standard deviations show that the location-weighting coefficients vary slightly for different test conditions. This might be caused by the variation of the still water level. When the water level is above the berm, the contribution of the roughness elements on the upper slope to the roughness influence might slightly decreases.

Since the location weighting coefficients are known, it is feasible to calculate the reductive influence of varying roughness. For example, the roughness factors for the waterside surface that have blocks applied on

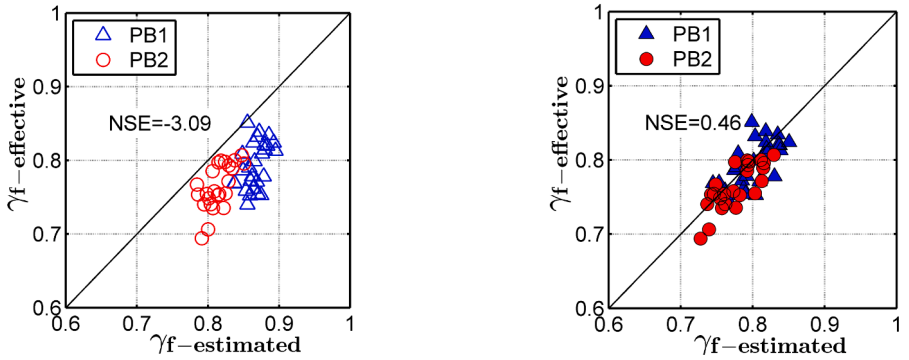

a) TAW equation (Eq. (1)) b) New equation (Eq. (6))

Fig. 10. Comparisons of effective roughness factors with estimated roughness factors of PB1 and PB2.

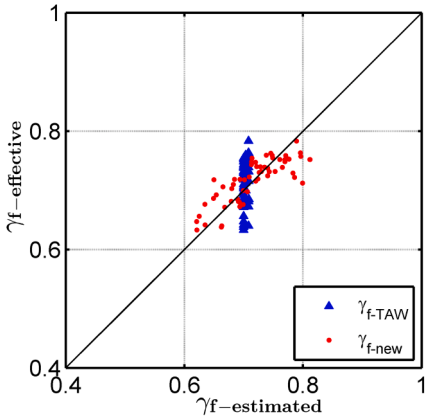

Fig. 11. Effective roughness factors vs estimated values using TAW (2002) method and the new equation for the roughness of open blocks on the straight slope.

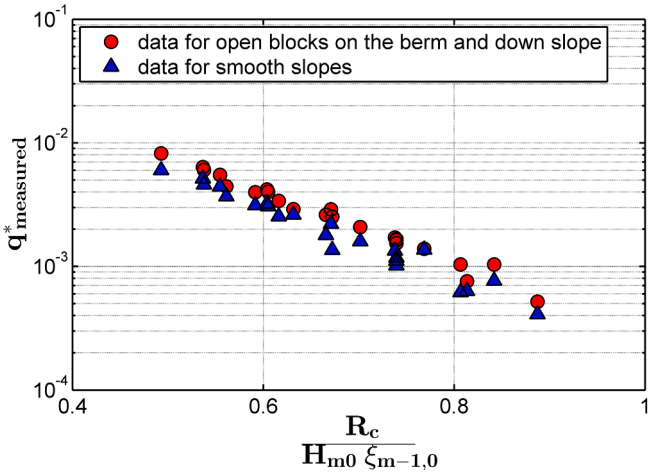

Fig. 12. Comparison of average overtopping discharges of section that has open blocks on the berm and down slope (OB2-d) and the section of smooth slopes that includes a berm (B-REF).

the upper slope in combination with a smooth berm and a smooth down slope can be calculated by using Eq. (7):

$$\gamma_f = \frac{0.65\gamma_{f-PB3}L_1 + 0.22{*}1{*}L_2 + 0.13{*}1{*}L_3}{0.65L_1 + 0.22L_2 + 0.13L_3} \tag{7}$$

where γ_{f-PB3} can be calculated by using Eq. (3). The effective roughness factors and calculated values by using Eq. (1) in which γ_{f-PB3} was calculated using Eq. (3) and by using the new equation (6) are compared in Fig. 10. Eq. (1) overestimates the combined roughness factors for PB1 and PB2. The new Eq. (6) performs much better in estimating the influence of varying roughness along the slopes with a berm with the NSE improving from −3.09 for Eq. (1) to 0.46 for the new equation.

3.3. Results for open blocks

The effective roughness factors of open blocks applied on the straight slope (Dataset S-OB) are calculated using the same method as applied in the calculation of the effective roughness factors of protruding blocks. The coefficient c_0 in Eq. (3) was recalibrated for open blocks by fitting the Dataset S-OB, which yields $c_{0,OB} = 0.38$. The roughness of open blocks is slightly larger than that of the protruding blocks with $c_{0,PB} = 0.36$.

Since 0.49 is not a reasonable value for open blocks on an impermeable core, it is recalibrated using the Dataset S-OB as 0.7 and is then used in comparison with the newly derived Eq. (3). Validation of the new equation for roughness of open blocks is performed by comparing the estimated roughness factors ($\gamma_{f-estimated}$) against the effective values ($\gamma_{f-effective}$), and an evident improvement over the TAW (2002) equation for the roughness influence is shown in Fig. 11 with NSE improving from 0.028 for the TAW (2002) equation to 0.39 for Eq. (3) with $c_{0,OB} = 0.38$.

The berm covered by open blocks with a 2.5 cm filter layer below the blocks is permeable. The observed overtopping discharges over section OB-2d with open blocks applied to the berm and down slope are larger than discharges of the smooth slopes that have a berm (B-REF) (see Fig. 12). This is counterintuitive since OB2-d is expected to be rougher. Possibly, also the permeability plays a role, which is in accordance with the results of a rock berm described in Krom (2012): who suggested that waves can to some extent propagate through a permeable berm leading to less energy reflection and less concentration of wave energy over the available water depth. Therefore, the permeable berms can be expected to result in less wave breaking than an impermeable berm. This could then lead to less wave dissipation due to wave breaking, and therefore a larger overtopping.

If the form of Eq. (5) for an impermeable berm is adopted for a permeable berm, then the γ_b should be larger for a permeable berm and consequently the empirical coefficient b_0 should be smaller than 0.21. Applying the equation for the roughness influence of open blocks on the straight slope to calculate the roughness factors of open blocks on the slopes that have a berm, results in a calibrated, b_0 of 0.22 using Dataset OB3. This is in contradiction with the observation that for permeable berms the influence of the berm is smaller than for an impermeable berm (since $b_0 = 0.22$ and not $b_0 < 0.21$). Therefore, the roughness influence equation for open blocks on the straight slope is not used for those

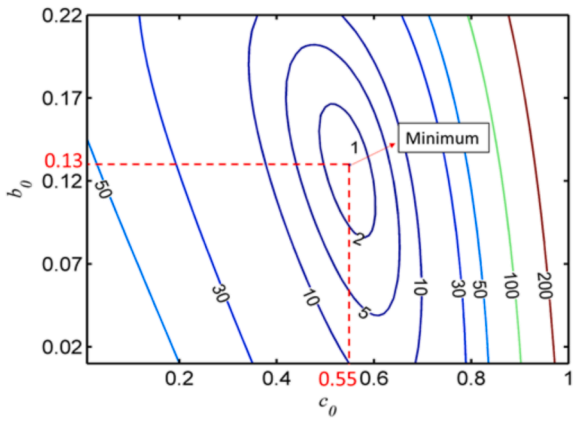

Fig. 13. Sum of the squares of the errors ε_i of overtopping data.

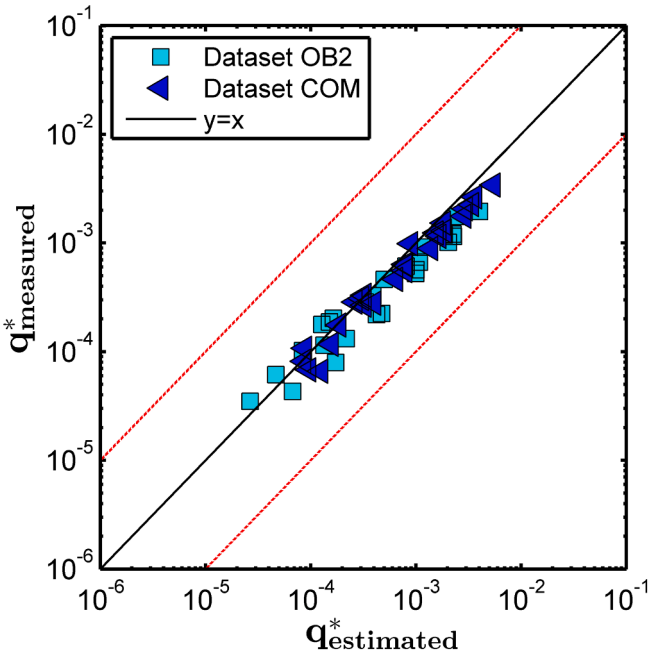

Fig. 14. Measured versus calculated dimensionless average overtopping discharges for: (1) section OB2 with open blocks applied on the upper slope and berm; and (2) section COM with protruding blocks on the upper slope and open blocks on the berm and down slope.

composite slopes that have a berm (section OB3). To derive the equations for the permeable berm influence and for the roughness influence of open blocks, the forms of Eq. (3) and (5) are applied with the coefficients b_0 and c_0 unknown. An important assumption made here is that the location weighting factors α_1, α_2 and α_3 proposed for protruding blocks are also applicable for open blocks on parts of the slopes that have a berm. Based on this assumption, Datasets OB1, OB2-d, OB3 are selected to calibrate coefficients b_0 and c_0 by using the method of least squares such that the sum of squares of the errors is at a minimum. The error is defined as:

$$\varepsilon_i = \log q^*_{i\_calculated} - \log q^*_{i\_measured} \tag{8}$$

Applying this procedure, we determine b_0 and c_0 as 0.13 and 0.55 respectively (Fig. 13). The standard errors of b_0 and c_0 are $6.74 \times 10^{-3}$and 4.70×10^{-3} respectively.

Datasets OB2 and COM are used to validate the assumption that we made and the new equations for open blocks. Fig. 14 shows that the measured and calculated overtopping discharges generally match well, which demonstrates the validity of the assumption and of the new derived equations for open blocks.

4. Discussion

4.1. New formulae for roughness and berm influence at dikes

The reductive effects of a berm and roughness on the average overtopping discharges at dikes were investigated by performing the proposed physical model tests for different slope configurations and wave conditions. Three new equations for berm and roughness influence factors (given in Box 1) are derived based on the analysis of the experimental results.

From the analysis of the roughness influence of protruding blocks and open blocks, we found that the roughness factors are not static values but are influenced by relative freeboard and breaker parameter. The empirical coefficient c_0 in Eq. (3) is related to the properties of roughness elements and dike configuration. For the open blocks, the value of c_0 for straight slopes is smaller than that for the slopes with a berm. This could be because the overtopping discharge is smaller due to the berm influence and therefore the open block revetment is rougher. In contrast, the values of c_0 for protruding blocks on the straight slopes and slopes with a berm are the same, which might be a coincidence. Hence, the coefficient c_0 is not necessarily the same for the straight slopes and for slopes with a berm. Figs. 6b and 10 show that Eq. (3) performs better than the TAW (2002) method. Moreover, Eq. (3) is straightforward and does not require an iterative calculation compared to the Capel (2015) roughness equation. It is feasible to adapt Eq. (3) to other types of roughness elements by calibrating the coefficient c_0.

The TAW equation for estimating the berm influence was modified by taking into account the wave steepness. The results showed that the berm influence decreases as the wave steepness increases. The permeable berm shows smaller reductions on the overtopping discharge than the impermeable berm. This is found by the experimental results showing that the overtopping discharges over section OB2-d are larger than B-REF under the identical wave conditions. Similarly, smaller overtopping discharges were also observed at section OB1 than at section OB3. A new equation was derived to calculate the berm influence factors with different values of the coefficient b_0 for impermeable and permeable berms. The coefficient b_0 should be a function of berm permeability and possibly other properties of the berm material. In this study, only three types of materials were considered. Therefore, we recommend to further investigate the berm influence by including larger variations of the permeability of the berm.

A new equation was developed to calculate the reductive influence of varying roughness along the slopes that have a berm. Roughness elements applied on the upper slope were more effective than those on the berm or down slope in reducing the overtopping discharges (Fig. 9). This phenomenon was also reported in Hunt-Raby et al. (2010).

Location-weighting coefficients α_1, α_2 and α_3 are introduced to describe the effect of applied locations of roughness elements on the overall roughness influence factors. In this study, coefficients α_1, α_2 and α_3 are determined to be 0.65, 0.22 and 0.13 for the upper slope, berm and down slope respectively, which clearly shows that the upper part has the largest weight. It should be noted that the still water levels in the tests were varied around the berm position within a narrow range of −0.03–0.03 m. The determined values of location weight factors are only valid within the tested ranges. Therefore, further investigation of the location weighting coefficients outside the tested ranges in this study are recommended.

4.2. Comparison with existing overtopping equations

The performance of the newly derived equations presented in this study is compared with three other overtopping formulae applicable for dikes among the full test data set (Fig. 15). The Capel (2015) method is

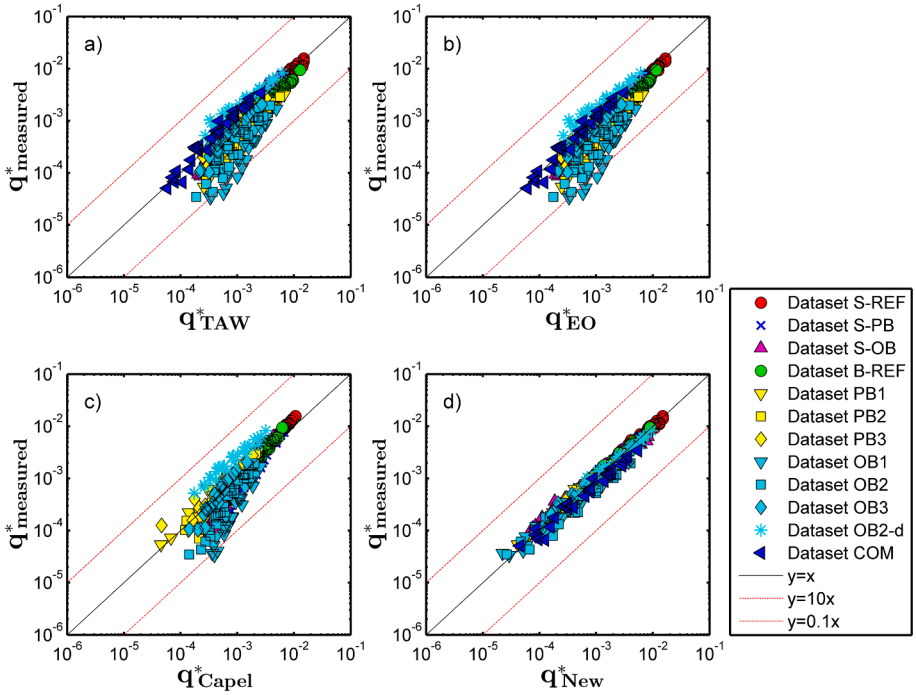

Fig. 15. Comparison between measured dimensionless overtopping discharges and calculated values by using a) TAW (2002), b) EurOtop, 2018 (EO), c) Capel (2015) and d) modified methods (New).

Table 2
Parameters of the selected datasets (Dataset A and B).

Parameters	Ranges
B [m]	0.4–1.0
H_{m0} [m]	0.1–0.2
d_h [m]	−0.08-0.13
R_c [m]	0.1–0.35
tan α[−]	1:3–1:4
$s_{m-1,0}$ [−]	0.024–0.05
$\xi_{m-1,0}$ [−]	1.10–1.55

only applicable for protruding blocks. Moreover, the Capel (2015) overtopping equation does not incorporate the berm influence factor γ_b. Therefore, the recalibrated value of 0.70 is applied to calculate the roughness factors of the open blocks in the extended Capel (2015) overtopping equation by the reductive factor for berms γ_b.

Fig. 15 shows a much better agreement between $q^*_{measured}$ and calculated q^* for the newly derived formulae compared with existing overtopping equations. The calculated statistical indicator NSE estimates are 0.72 (TAW, 2002), 0.71 (EurOtop, 2018), 0.78 (Capel, 2015) and 0.97 (new formulae), which shows that the newly derived formulae for berms and roughness perform better than the existing methods within the tested ranges. The Capel (2015) method gives a better estimation of the overtopping discharges than other existing equations since the method takes into account the variation of roughness factors of protruding blocks with wave conditions and blocks applied on parts of

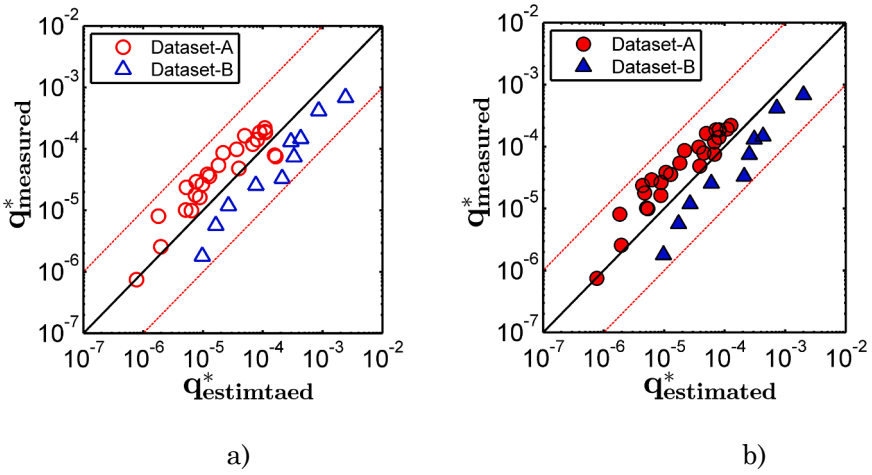

Figure 16. $q^*_{measured}$ versus $q^*_{calculated}$ using a) TAW (2002) method and b) new equation of impermeable berm influence using selected data recordings from Van der Meer and De Waal (1990) and Van der Meer and De Waal (1993).

Box 1
Summary of derived formulae in this study

Berm influence factor

$$\gamma_b = 1 - \left(b_0 \Big/ \sqrt{s_{m-1,0}}\right) r_B (1 - r_{dh})$$

with $b_0 = 0.21$ for an impermeable berm and $b_0 = 0.13$ for a permeable berm covered by open blocks.

Roughness influence factor

$$\gamma_f = 1 - c_0 R_c \Big/ \left(H_{m0} \xi_{m-1,0}\right)$$

with $c_0 = 0.36$ for protruding blocks on the straight slopes and composite slope slopes with a berm; $c_0 = 0.38$ for open blocks on the straight slope and $c_0 = 0.55$ for open blocks on the slopes with a berm.

Varying roughness along the slopes and berm

$$\gamma_f = \left(\alpha_1 \gamma_{f,1} L_1 + \alpha_2 \gamma_{f,2} L_2 + \alpha_3 \gamma_{f,3} L_3\right) \Big/ \left(\alpha_1 L_1 + \alpha_2 L_2 + \alpha_3 L_3\right)$$

with $\alpha_1 = 0.65$ for the upper slope, $\alpha_2 = 0.22$ for the berm and $\alpha_3 = 0.13$ for the down slope.

the slope surface. However, Capel (2015) equation cannot deal with the roughness of the combination of protruding blocks and other types of armour units. EurOtop (2018) performs similarly with the TAW (2002) within the calibration set.

4.3. Validation of new berm influence equation

The equation to account for the influence of berms on the wave overtopping discharges has been based on the present data-set. To show its validity beyond the tested ranges, Eq. (5) has been compared to existing data for smooth impermeable slopes. Two datasets A and B (Van der Meer and De Waal, 1990; Van der Meer and De Waal, 1993) were used for this purpose; the ranges of parameters in these two datasets are listed in Table 2. Measured and calculated dimensionless overtopping discharges are plotted in Fig. 16. The new equation performs similarly with *NSE* = 0.53 for Dataset A and *NSE* = 0.57 for Dataset B compared with the TAW (2002) method with *NSE* = 0.58 for Dataset A and NSE = 0.52 for Dataset B. One reason for the similar performance of both methods is that the minimum value of berm factor is 0.6. This implies that, if the calculated value is less than 0.6, the value 0.6 is used. The new method also adopts this specification. Most of Datasets A and B resulted in berm influence factors smaller than 0.6 due to a large berm width and therefore both the new and TAW methods give the same values for the berm factor. The relatively low NSE values for both the TAW (2002) formulas and the new formula indicate that additional research is needed to determine the berm factors for very wide berms.

4.4. Scale effects

Scale effects cannot be avoided when performing scaled model tests (EurOtop (2018)). This is because it is impossible to fulfil Froude's law and Reynold's law at the same time to obtain completely reliable results from scaled models. Froude scaling is important for a scale reproduction of waves since the inertia and gravity are the dominant forces in flows related to waves. The consequence of Froude modelling is that viscous forces are high in the model if identical fluids are used in both the prototype and the model. Previous research (Schüttrumpf, 2001) has shown that the influence of kinematic viscosity on wave overtopping increases as the overtopping discharges decrease. Small-scale model tests tend to give smaller values of overtopping rates compared to those of large-scale model tests (Kajima and Sakakiyama, 1994). There is a tendency of rougher behaviour of revetments for small overtopping quantities below 0.4 l/s/m in prototype scale compared with the real cases (Capel, 2015). De Rouck et al. (2005) showed that results of model and prototype are in relatively good agreement for relatively larger overtopping discharges. The vast majority of the data in the present study corresponds to larger overtopping discharges (>0.4 l/s/m). Therefore, viscous forces have not caused significant scale effects on wave overtopping discharge in this study.

5. Conclusions

In this study 429 tests were performed to determine the influence of a berm and roughness on the wave overtopping over dikes. Based on the analysis of the model tests, new formulae have been derived to estimate the reduction of wave overtopping at dikes due to the roughness, due to a berm, and a combination of both.

We found that roughness influence factors appear not to be constant as assumed by TAW (2002) and EurOtop (2007, 2018) but vary in response to the wave conditions and dike configurations. The wave steepness is included in the new equation in addition to the relative berm width and the berm level to improve the accuracy of predicting the berm influence. This new formula to take the influence of berms into account has been validated against existing data and was found to perform similarly with the TAW (2002) method. Experimental results suggest that a permeable berm has a slightly smaller reductive influence than an impermeable berm. Location-weighting coefficients are applied to account for the different contributions of roughness elements on different parts of the waterside slopes to the overall roughness influence factor. This method can be used to estimate the reduction influence of varying roughness along the slopes and the berm.

The new formulae derived as listed in Box 1 in this study fit well with the experimental data with NSE of 0.97 and perform better than existing formulae to predict average overtopping discharges within the calibration set. This improvement is obtained by using variable roughness coefficients and by taking wave steepness into account when calculating berm coefficients. Also, the location-weighting coefficients for roughness elements contribute to the improvement of overtopping estimation. The restricted calibration dataset is probably the reason of the poor result of validation with two datasets (A and B) which are not used in the calibration. It is recommended to further validate these new formulae with more extensive data being available.

Acknowledgement

The first author thanks the China Scholarship Council for providing the research grant. This work is also part of the All-Risk research programme, with project number P15-21, which is partly financed by the

Netherlands Organisation for Scientific Research (NWO). The model technicians of Deltares are thanked for their contributions to the physical model tests.

Appendix A

Appendix A.1. Empirical overtopping formulae

TAW (2002) provides the overtopping formulae for breaking and non-breaking waves as given below:

$$\frac{q}{\sqrt{gH_{m0}^3}} = \frac{0.067}{\sqrt{\tan\alpha}}\gamma_b\xi_{m-1,0}\exp\left(-4.75\frac{R_c}{H_{m0}\xi_{m-1,0}\gamma_b\gamma_f\gamma_\beta\gamma_v}\right) \tag{A.1}$$

with a maximum of

$$\frac{q}{\sqrt{gH_{m0}^3}} = 0.2\exp\left(-2.6\frac{R_c}{H_{m0}\gamma_f\gamma_\beta}\right) \tag{A.2}$$

where q [m^3/s/m] is the average overtopping discharge, R_c [m] is the freeboard which is the vertical distance of the dike crest relative to the Still Water Level (SWL), $\xi_{m-1,0}$ (=tanα/$\sqrt{2\pi H_{m0}/gT_{m-1,0}^2}$) is the breaker parameter, γ_b [−] is the influence factor for berms, γ_f [−] is the roughness factor, γ_β [−] is the influence factor for oblique waves, γ_v [−] is the influence factor for vertical walls. The other empirical overtopping formulae are shown in Table A.1, where G_c is the width of armour crest [m].

Table A.1
Summary of the empirical overtopping formulae.

Reference	Formula
TAW (2002)	$\frac{q}{\sqrt{gH_{m0}^3}} = \frac{0.067}{\sqrt{\tan\alpha}}\gamma_b\xi_{m-1,0}\exp\left(-4.75\frac{R_c}{H_{m0}\xi_{m-1,0}\gamma_b\gamma_f\gamma_\beta\gamma_v}\right)$ with the maximum of $\frac{q}{\sqrt{gH_{m0}^3}} = 0.2\exp\left(-2.6\frac{R_c}{H_{m0}\gamma_f\gamma_\beta}\right)$
EurOtop et al. (2018)	$\frac{q}{\sqrt{gH_{m0}^3}} = \frac{0.023}{\sqrt{\tan\alpha}}\gamma_b\xi_{m-1,0}\exp\left[-\left(2.7\frac{R_c}{\xi_{m-1,0}H_{m0}\gamma_b\gamma_f\gamma_\beta\gamma_v}\right)^{1.3}\right]$ with the maximum of $\frac{q}{\sqrt{gH_{m0}^3}} = 0.09\exp\left[-\left(1.5\frac{R_c}{H_{m0}\gamma_f\gamma_\beta\gamma^*}\right)^{1.3}\right]$
Capel (2015)	$\frac{q}{\sqrt{gH_{m0}^3}} = \frac{0.027}{\sqrt{\tan\alpha}}\xi_{m-1,0}\exp\left[-\left(6.5\frac{R_c}{3.45\tanh(0.65\xi_{m-1,0})H_{m0}\gamma_f}\right)\right]$

Appendix A.2. Berm influence equation

TAW (2002) and EurOtop (2007, 2018) recommend a method to calculate the berm influence factors.

$$\gamma_b = 1 - r_B(1 - r_{dh}) \text{ if } 0.6 \le \gamma_b \le 1.0 \tag{A.3}$$

$$r_B = \frac{B}{L_{Berm}}$$

$$r_{dh} = 0.5 - 0.5\cos\left(\pi\frac{d_h}{R_{u2\%}}\right) \text{ for a berm above still water line}$$

$$r_{dh} = 0.5 - 0.5\cos\left(\pi\frac{d_h}{2H_{m0}}\right) \text{ for a berm below still water line}$$

In which $R_{u2\%}$ is the wave run-up height exceeded by 2% of the incident waves and it can calculated by using the following equations (TAW, 2002):

$$\frac{R_{u2\%}}{H_{m0}} = 1.65\gamma_b\gamma_f\gamma_\beta\xi_{m-1,0} \text{ with } \xi_{m-1,0} = \frac{\tan\alpha}{\sqrt{s_{m-1,0}}} \tag{A.4}$$

with a maximum of

$$\frac{R_{u2\%}}{H_{m0}} = \gamma_f\gamma_\beta\left(4 - \frac{1.5}{\sqrt{\xi_{m-1,0}}}\right) \tag{A.5}$$

where r_B[−] represents the influence of the width B[m] and r_{dh}[−] stands for the effect of the d_h[m] which refers to position of the berm relative to SWL, L_{Berm}[m] is the characteristic berm length (Fig. A.1).

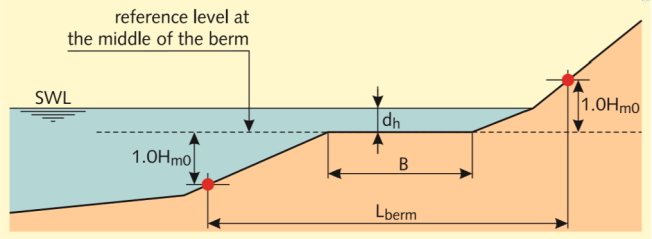

Fig. A.1. Definition of the berm of a dike (from TAW, 2002).

Appendix A.3. Roughness influence equation

The method given by TAW (2002) and EurOtop (2007, 2018) to account for roughness can be described as below:

$$\gamma_f = \begin{cases} \gamma_{f-rec} & if\ \gamma_b\xi_{m-1,0} < 1 \\ \gamma_{f-rec} + (\gamma_b\xi_{m-1,0} - 1.8)\cdot\dfrac{1-\gamma_{f-rec}}{8.2} & if\ 1.8 < \gamma_b\xi_{m-1,0} < 10 \\ 1.0 & if\ \gamma_b\xi_{m-1,0} > 10 \end{cases} \tag{A.6}$$

in which γ_{f-rec}[−] refer to the recommended values of the roughness factor by TAW (2002) and EurOtop (2007, 2018).

A new equation to assess the roughness influence coefficient of protruding blocks was proposed by Capel (2015).

$$\gamma_f = 1 - \left\{ 0.585 \cdot \sqrt{0.075 - s_{m-1,0}^{\cdot}} \cdot \sqrt{\rho_{\gamma_f}} \cdot \left[-\ln\left(\frac{q}{\sqrt{gH_s^3}} \right) \right] \right\} \tag{A.7}$$

with

$$\rho_{\gamma_f} = \frac{\gamma_{f,w}\cdot\sin\alpha\cdot h_{prot}}{R_c} \tag{A.8}$$

where $s_{m-1,0}^{\cdot}$[−] is the local wave steepness; ρ_{γ_f}[−] is the roughness density parameter; H_s [m] is the significant wave height; $\gamma_{f,w}$[−] is the dimensionless roughness width, which refers to the total width of the exposed elements per meter dike; h_{prot}[m] is the protrusion height.

References

Borsje, B.W., van Wesenbeeck, B.K., Dekker, F., Paalvast, P., Bouma, T.J., van Katwijk, M.M., de Vries, M.B., 2011. How ecological engineering can serve in coastal protection. Ecol. Eng. 37, 113–122.

Bruce, T., Van der Meer, J.W., Franco, L., Pearson, J.M., 2009. Overtopping performance of different armour units for rubble mound breakwaters. Coast. Eng. 56, 166–179.

Capel, A., 2015. Wave run-up and overtopping reduction by block revetments with enhanced roughness. Coast. Eng. 104, 76–92. https://doi.org/10.1016/j.coastaleng.2015.06.007.

De Rouck, J., Geeraerts, J., Troch, P., Kortenhaus, A., Pullen, T., Franco, L., 2005. New results on scale effects for wave overtopping at coastal structures. In: Proc. int. conf. coastalines, struct. break., pp. 1–14.

EurOtop, 2007. Wave Overtopping of Sea Defences and Related Structures–Assessment Manual. UK NWH Allsop. T. Pullen, T. Bruce. NL JW van der Meer. H. Schüttrumpf, A. Kortenhaus. http://www.overtopping-manual.com.

EurOtop, 2018. Manual on Wave Overtopping of Sea Defences and Related Structures, an Overtopping Manual Largely Based on European Research, but for Worldwide Application. Van der Meer, J.W., Allsop, N.W.H, Bruce, T., De Rouck, J., Kortenhaus, A., Pullen, T., Schüttrumpf, H., Troch, P., Zanuttigh, B. www.overtopping-manual.com.

Gallach-Sánchez, D., 2018. Experimental Study of Wave Overtopping Performance of Steep Low-Crested Structures. PhD Thesis. Universiteit Gent.

Goda, Y., 2009. Derivation of unified wave overtopping formulas for seawalls with smooth, impermeable surfaces based on selected CLASH datasets. Coast. Eng. 56, 385–399. https://doi.org/10.1016/j.coastaleng.2008.09.007.

Hunt-Raby, A., Othman, I.K., Jayaratne, R., Bullock, G., Bredmose, H., 2010. Effect of protruding roughness elements on wave overtopping. In: Coasts, Marine Structures and Breakwaters: Adapting to Change: Proceedings of the 9th International Conference Organised by the Institution of Civil Engineers and Held in Edinburgh on 16 to 18 September 2009. Thomas Telford Ltd, pp. 2–574.

Jafari, E., Etemad-Shahidi, A., 2011. Derivation of a new model for prediction of wave overtopping at rubble mound structures. J. Waterw. Port, Coast. Ocean Eng. 138, 42–52.

Kajima, R., Sakakiyama, T., 1994. Review of works using CRIEPI flume and present work. In: Coastal Dynamics94. ASCE, pp. 614–627.

Krom, J., 2012. Wave Overtopping at Rubble Mound Breakwaters with a Non-reshaping Berm. Master thesis. Delft Univ. Technol.

Mansard, E.P.D., Funke, E.R., 1980. The measurement of incident and reflected spectra using a least squares method. Coast Eng. 154–172, 1980.

Pillai, K., Etemad-Shahidi, A., Lemckert, C., 2017. Wave overtopping at berm breakwaters: experimental study and development of prediction formula. Coast. Eng. 130, 85–102. https://doi.org/10.1016/j.coastaleng.2017.10.004.

Schüttrumpf, H., 2001. Wellenüberlaufströmung an Seedeichen: Experimentelle und theoretische Untersuchungen. PhD Thesis. Braunschweig University.

TAW, 2002. Technical Report Wave Run-Up and Wave Overtopping at Dikes. Technical Advisory Committee on Flood Defence, Delft, The Netherlands.

Temmerman, S., Meire, P., Bouma, T.J., Herman, P.M.J., Ysebaert, T., De Vriend, H.J., 2013. Ecosystem-based coastal defence in the face of global change. Nature 504, 79.

Van der Meer, J.W., De Waal, J.P., 1993. Waterbeweging op taluds, Invloed van berm, ruwheid, ondiep voorland en scheve lang- en kortkammige golfaanval. Waterloopkundig Laboratorium, Verslag, p. H1256 (in Dutch).

Van der Meer, J.W., De Waal, J.P., 1990. Invloed van scheve inval en richtingspreiding op golfoploop en overslag. Waterloopkundig Laboratorium, Verslag modelonderzoek, p. H638 (in Dutch).

Van Gent, M.R.A., 2013. Rock stability of rubble mound breakwaters with a berm. Coast. Eng. 78, 35–45.

Van Gent, M.R.A., 1999. Physical Model Investigations on Coastal Structures with Shallow Foreshores: 2D Model Tests on the Petten Sea-Defence. Delft Hydraul. Rep. H3129, Delft.
Van Gent, M.R.A., Plate, S.E., Berendsen, E., Spaan, G.B.H., Van Der Meer, J.W., d'Angremond, K., 1999. Single-layer rubble mound breakwaters. In: Proc. Coastal Structures.
Van Gent, M.R.A., Van den Boogaard, H.F.P., Pozueta, B., Medina, J.R., 2007. Neural network modelling of wave overtopping at coastal structures. Coast. Eng. 54, 586–593.
Van Steeg, P., Joosten, R.A., Steendam, G.J., 2018. Physical model tests to determine the roughness of stair shaped revetments. In: 3th Int. Conf. Prot. Against Overtopping, pp. 1–8. UK.
Verhaeghe, H., De Rouck, J., van der Meer, J., 2008. Combined classifier–quantifier model: a 2-phases neural model for prediction of wave overtopping at coastal structures. Coast. Eng. 55, 357–374.

List of symbols

α: : angle of the waterside slope of a dike
α_1: : location-weighting factor for the upper slope
α_2: : location-weighting factor for the berm
α_3: : location-weighting factor for the down slope
ε_i: : difference between the measured and calculated overtopping discharge [−]
γ_f: : roughness influence factor [−]
γ_b: : berm influence factor [−]
γ_v: : influence factor of a vertical wall [−]
γ_β: : influence factor of oblique waves [−]
$\xi_{m-1,0}$: : breaker parameter [−]
b_0: : empirical coefficient for the berm influence factor [−]
B: : berm width [m]
c_0: : empirical coefficient for the roughness influence factor [−]
H_{m0}: : spectral significant wave height [m]
$T_{m-1,0}$: : spectral wave period [s]
$s_{m-1,0}$: : wave steepness [−]
r_B: : influence of berm width [−]
R_c: : level of dike crest relative to the still water line [m]
r_{dh}: : influence of berm level [−]
d_h: : water depth above the berm [m]
q: : mean overtopping discharge [l/s/m]
q^*: : dimensionless mean overtopping discharge [−]
l: : total coverage length of roughness elements on the surface [m]
L_1: : effective coverage length of the roughness elements on the upper slope [m]
L_2: : effective coverage length of the roughness elements on the berm [m]
L_3: : effective coverage length of the roughness elements on the down slope [m]
L_{Berm}: : berm length [m], refer to Fig. A.1
$R_{u2\%}$: : wave run-up height, exceeded by 2% of the incident waves [m]